Closed Loop Carrier Phase Synchronization Techniques Motivated by Likelihood Functions:

Haiping Tsou, Member IEEE
Marvin Simon, Fellow IEEE
Sami Hinedi, Member IEEE

Abstract

This paper reexamines the notion of closed loop carrier phase synchronization motivated by the theory of maximum a posteriori (MAP) phase estimation with emphasis on the development of new structures based on both maximum-likelihood (ML) and average-likelihood (AL) functions. The criterion of performance used for comparison of all the closed loop structures discussed is the mean-squared phase error for a fixed loop bandwidth. For low SNR applications, a closed loop structure motivated by a particular interpretation of the ML function is shown to outperform the so-called I-Q MAI? estimation loop which is motivated by AL considerations and which itself outperforms other well-known loops such as the I-Q Costas loop and I-Q polarity-type Costas loop.

‘This work was performed by the Jet Propulsion Laboratory, California Institute of Technology, under a contract with the National Aeronautics and Space Administration.

Closed Loop Carrier Phase Synchronization Techniques Motivated by Likelihood Functions

Haiping Tsou, Section 331
Marvin Simon, Section 339
Sami Hinedi, Section 331

1.0 Introduction

It is well known [1] that estimation of an unknown parameter based on a likelihood function approach is optimum in the sense of maximizing the à posteriori probability of the parameter given the observation. For the case where the unknown parameter is the random phase of a carrier received in a background of additive white Gaussian noise (AWGN), optimum open loop structures have been derived for implementing the resulting phase estimate [2,3]. Herein, these structures are referred to as *open loop carrier phase estimators.*

When the carrier is unmodulated and its frequency is known, then its phase is the only unknown parameter. As such, the optimum phase estimate is obtained by first evaluating the a posteriori probability of the carrier phase given an observation of the received carrier plus noise and then finding the value of carrier phase (often called the *maximum a posteriori (MAP) phase estimate)* that maximizes this function. Since when the carrier phase is unknown, it is assumed to be uniformly distributed in the interval $(-\pi,\pi)$, then from Bayes' rule one can equivalently maximize the conditional probability density function (pdf) of the observation given the carrier phase. The phase estimate that results from this maximization is usually called the *maximum-likelihood phase* estimate. For reasons that will become apparent shortly, we shall reserve this terminology for another meaning.

When the carrier is data-modulated, then the above conditional pdf depends, in addition, on the data sequence that exists during the interval of observation for the received signal. Hence, before maximizing this function with respect to the carrier phase, one has to choose how to eliminate its dependence on the unknown data sequence, If one is only interested in determining the optimum carrier phase estimate, then the appropriate choice is to *average* the conditional pdf over the unknown data sequence. We shall refer to the phase estimate obtained by this process as the *average-likelihood (AL)* estimate. If, however, one is interested in joint phase estimation and data detection, then the appropriate choice is to first *maximize* the conditional pdf with respect to the data sequence (resulting in the most probable sequence), and then maximize it with respect to the carrier phase.[1] We shall refer to the phase estimate obtained by this process as the *maximum-likelihood (ML)* estimate.[2] It has often been conjectured, although never proven, that from the standpoint of phase estimation alone, the ML phase estimate is suboptimum to the AL estimate. Because of this, what is typically done in practice is to derive the AL carrier phase estimate and then use this estimate as the phase of a demodulation reference signal for performing bit by bit data detection. However, it should be understood that, from the standpoint of joint estimation of data and carrier phase, this sequential operation of ***first*** deriving the carrier phase estimate in the absence of any knowledge of the data (the AL approach) and *then* detecting the ensuing data using the phase estimate so derived is, in general, suboptimum.

Aside from the optima lit y of the AL and ML approaches to open loop estimation of carrier phase, likelihood functions have also been used as *motivation* for closed loop carrier phase synchronization. Emphasis is placed on the word motivation since indeed there is no guarantee that the resulting closed loop schemes are optimal nor can one guarantee that those schemes motivated by the AL approach will outperform those motivated by the ML approach (although typically this turns out to be the case). Nonetheless, as we shall see, closed loop carrier phase estimation schemes motivated by likelihood functions do indeed yield good tracking performance (as measured by the mean-squared value of the loop phase error). In fact, under suitable assumptions, many of them are synonymous with well-known carrier tracking loops, e.g., the *I-Q Costas loop* and the *I-Q decision feedback* or *polarity-type Costas loop* [4,5] that have been around for many decades.

It is the intent of this paper to explore in more detail the structure and performance of closed loop carrier phase synchronization loops motivated by likelihood functions. Before proceeding with the mathematical details, it is important to define the meaning of the term "closed loop phase estimation scheme motivated by the likelihood function approach." As stated above, in the open loop case, the optimum phase estimate is that value of carrier phase that maximizes the conditional

[1] In principle, the order of maximization operations could be reversed.

[2] In the strictest of parlance, both the AL and the ML phase estimates are maximum-likelihood estimates since the term "maximum-likelihood estimation" is typically reserved for estimating a purely unknown (uniformly distributed) random parameter. However, to allow for distinguishing between the two different ways in which the data sequence is handled, we shall use the above terminology.

pdf of thereceived observation given the carrier phase. Analternate wayof saying the same thing is that the optimum open loop phase estimate is the "value of phase at which the derivative of this same conditional pdf equates to zero. Using this interpretation of the optimum phase estimate, we make the observation that in the neighborhood of this zero slope point, the magnitude and polarity of the conditional pdf's derivative would respectively represent an indication of how far away and in which direction (i.e., less than or greater than) one is from the true optimum phase estimate. As such, it is suggested that the derivative (or some monotonic function of derivative) of the above conditional pdf be used as an *error signal* in a closed loop phase estimation scheme. It is in this context that we talk about closed loops motivated by likelihood functions. Herein, for the purpose of abbreviated notation, we shall refer to such loops as AL and ML closed loops depending on the particular likelihood function used to define the error signal.

It is important at this point to mention that the notion of closed loops based on likelihood functions as per the above definition is indeed not new and one should not attribute its originality to the authors of this paper. Rather the purpose of this paper is to expand upon this notion and present some new loops motivated by likelihood functions along with their tracking performance. As such, we are not reinventing the wheel but rather adding some more spokes to it.

2.0 System Model

Consider a system that transmits BPSK[3] modulation over an AWGN channel. As such the received signal takes the form

$$r(t) = \sqrt{2S}d(t)\sin\left(\omega_c t + \theta\right) + n(t) \tag{1}$$

where S denotes the received power, ω_c is the carrier frequency in rad/see, θ is the unknown phase assumed to be uniformly distributed in the interval $(-\pi, \pi)$, $n(t)$ is an the AWGN with single-sided power spectral density N_0 watts/Hz, and d(t) is a binary-valued (± 1) random pulse train defined by the rate 1/T binary data sequence $\{d_i\}$ and the rectangular pulse shape, $p(t)$, as

$$d(f) = \sum_{i=-\infty}^{\infty} d_i p(t - iT), \quad p(f) = \begin{cases} 1; & 0 \le t \le T \\ 0; & \text{otherwise} \end{cases} \tag{2}$$

For an observation interval of L bits [we assume without loss of generality the interval

[3]We restrict ourselves to the case of binary modulation. By a straightforward extension of the procedures discussed, the results can easily be extended to M-ary modulation.

$(0, LT)]$, the conditional pdf of the received signal (observation) given the unknown phase and the particular data sequence, d_i, transmitted in that interval is easily shown to be

$$p\left(r(t)\middle|d_i(t),\theta\right) = C_0 \exp\left(\frac{2\sqrt{2S}}{N_0}\int_0^{LT} r(t)d_i(t)\sin\left(\omega_c t + \theta\right)dt\right) \triangleq q_i(\theta) \qquad (3)$$

where $d_i(t)$ is the transmitted waveform corresponding to the transmitted sequence in accordance with (2) and C_0 is a constant of proportionality. To proceed further, we must now choose between AL and ML approaches,

3.0 <u>Closed LooPs Motivated bv the AL Approach</u>
3.1 <u>Structures</u>

Suppose that we are interested only in estimating the carrier phase, 8. Then, as previously mentioned, the appropriate approach is to average $p\left(r(t)\middle|d_i(t), 8\right)$ over all possible (2^L) and equally likely data sequences yielding the conditional pdf

$$p\left(r(t)\middle|\theta\right) = \frac{1}{2^L}\sum_{i=1}^{2^L} p\left(r(t)\middle|d_i(t),\theta\right) = C_1\sum_{i=1}^{2^L}\exp\left(\frac{2\sqrt{2S}}{N_0}\int_0^{LT} r(t)d_i(t)\sin\left(\omega_c t + \theta\right)dt\right) \triangleq q(\theta) \qquad (4)$$

where C_1 is again a constant of proportionality. One AL open loop phase estimate (herein referred to as *AL open loop estimator #1*) is obtained by finding the value of θ that maximizes $q(\theta)$ of (4), i.e.,

$$\hat{\theta} \triangleq \max_{\theta}^{-1}\sum_{i=1}^{2^L}\exp\left(\frac{2\sqrt{2S}}{N_0}\int_0^{LT} r(t)d_i(t)\sin\left(\omega_c t + \theta\right)dt\right) \qquad (5)$$

where the inverse maximum notation "$\max^{-1} f(\theta)$" denotes the value of θ that maximizes $f(\theta)$. A block diagram implementation of this estimator is illustrated in Figure la,

Alternately, breaking up the integration over the entire observation into a sum of integrals on each bit interval and recognizing that the data bits are independent identically distributed (iid) binary random variables, then (4) evaluates to

$$p\left(r(t)\middle|\theta\right) \cdot C_2\prod_{k=0}^{L-1}\cosh\left(\frac{2\sqrt{2S}}{N_0}\int_{kT}^{(k+1)T} r(t)\sin\left(\omega_c t + \theta\right)dt\right) \triangleq v(\theta) \qquad (6)$$

A second AL open loop phase estimate (herein referred to as *AL open loop estimator #2) is* obtained by finding the value of θ that maximizes v(O) of (6), i.e.,

$$\hat{\theta} \triangleq \max_{\theta}^{-1} \prod_{k=0}^{L-1} \cosh\left(\frac{2\sqrt{2S}}{N_0}\int_{kT}^{(k+1)T} r(t)\sin(\omega_c t + \theta)dt\right) \tag{7}$$

A block diagram implementation of this estimator is illustrated in Figure lb.

Finally, one could obtain an AL open loop estimator by maximizing *any* monotonic function of v(0), for example in v(O). The reason for choosing the natural logarithm as the monotonic function is to simplify the mathematics, i.e., to convert the L-fold product in (7) to an L-fold sum. Thus, the third AL open loop phase estimate (herein referred to as *AL open loop estimator* #3) is obtained by finding the value of θ that maximizes ln v(O), namely,

$$\hat{\theta} \triangleq \max_{\theta}^{-1} \sum_{k=0}^{L-1} \ln\cosh\left(\frac{2\sqrt{2S}}{N_0}\int_{kT}^{(k+1)T} r(t)\sin(\omega_c t + \theta)dt\right) \tag{8}$$

A block diagram implementation of this estimator is illustrated in Figure 1c and is the form most commonly found in discussions of open loop MAP carrier phase estimation.

Before proceeding to the AL closed loop structures, it is important to emphasize that the three AL open loop phase estimates as described by (5), (7), and (8) are identical. That is, even though the functions $q(\theta)$, v(O), and in $v(\theta)$ are totally different, the values of θ at which each achieves its maximum are all the same. Thus, from the standpoint of finding the optimum open loop phase estimate, it makes no difference which of the three structures in Figure 1 is implemented, i.e., they all yield the same performance. As we shall see shortly, this same statement is *not* true when considering the performances of the closed loops motivated by these three different AL formulations. Stated another way, optimally equivalent open loop phase estimates produced by equivalent AL functions do not necessarily produce optimally equivalent closed loop phase tracking structures. In fact, for a *given* AL formulation, e.g., #1, #2, or #3, optimality of the open loop phase estimator in no way guarantees optimality of the closed loop structure.

A closed loop phase synchronization structure[4] based on AL open loop estimator #1 is illustrated in Figure 2a where, in accordance with the discussion given in the introduction, the error signal, e, is given by [see Eq. (5)]

[4]For ease of illustration, we show only the portion of the closed loop that generates the loop error signal which in the actual implementation becomes the input to the loop filter.

$$\sigma_\phi^2 = \frac{1}{\rho}\left[\frac{L\sum_{i=1}^{2^L}\sum_{j=1}^{2^L} D_{ij}\exp\left\{2R_d\left(L + D_i + D_j + D_{ij}\right)\right\}}{\left[\sum_{m=0}^{L}\binom{L}{m}(L-2m)\exp\left\{\left(R_d(3L-4m)\right)\right\}\right]^2}\right] \triangleq \frac{1}{\rho S_L} \tag{12}$$

where

$$\rho = \frac{S}{N_0 B_L}, \qquad R_d = \frac{ST}{N_0} \tag{13}$$

and

$$D_i = \sum_{k=0}^{L-1} d_k d_{ik}, \; D_{ij} = \sum_{k=0}^{L-1} d_{ik} d_{jk} \tag{14}$$

with

$$\begin{aligned} \mathbf{d} &\triangleq (d_0, d_1, \ldots, d_{L-1}) = \text{transmitted data sequence} \\ \mathbf{d}_i &\triangleq (d_{i0}, d_{i1}, \ldots, d_{i,L-1}) = i\text{th data sequence}; \quad i = 1,2,\ldots,2^L \end{aligned} \tag{15}$$

In (12), D_i represents the correlation of the ith data sequence with the transmitted sequence and D_{ij} represents the correlation between the ith and the jth data sequences. Some properties of D_i and D_{ij} that are particularly useful in obtaining many of the results that follow are summarized in Table I. The factor S_L represents the loss of the *effective* loop SNR, $\rho' \triangleq \sigma_\phi^{-2}$, relative to the loop SNR, ρ, of a phase-locked loop (PLL). For certain configurations, as we shall see, this loss is synonymous with what is commonly referred to as *squaring loss* [4, 8].

At first glance, it might appear that, for given values of ρ, R_d, and the observation length; L, the mean-squared phase error would be a function of the particular sequence chosen as the transmitted sequence. It is easy to show that indeed this is not the case, i.e., σ_ϕ^2 is independent of the sequence selected for d .[6] To see this, consider a sequence $\mathbf{d}_l \triangleq (d_{l0}, d_{l1}, \ldots, d_{l,L-1}) \neq \mathbf{d}$ and rewrite D_i and D_{ij} as

---

[6]For convenience of evaluation of (12), we may choose the all 1's sequence for d in which case D_i simplifies to $\sum_{k=0}^{L-1} d_{ik}$ which takes on values $L-2m$, $m = 0, 1, 2, \ldots, L$.

$$e \triangleq \frac{dq(\theta)}{d\hat{\theta}} = \sum_{i=1}^{2^L} \left(\exp\left(\frac{2\sqrt{2S}}{N_0} \int_0^{LT} r(t) d_i(t) \sin(\omega_c t + \theta) dt \right) \right) \left[\frac{2\sqrt{2S}}{N_0} \int_0^{LT} r(t) d_i(t) \cos(\omega_c t + \theta) dt \right) \tag{9}$$

Analogous closed loop phase synchronization structures corresponding to AL open loop estimators #2 and #3 are illustrated in Figures 2band 2cwhere the error signals are respectively given by [see Eq. (7)and (8)1

$$e \triangleq \frac{dv(\theta)}{d\theta} = \prod_{k=0}^{L-1} \cosh\left(\frac{2\sqrt{2S}}{N_0} \int_{kT}^{(k+1)T} r(t) \sin(\omega_c t + \theta) dt \right)$$
$$\times \sum_{k=0}^{L-1} \left(\tanh\left(\frac{2\sqrt{2S}}{N_0} \int_{kT}^{(k+1)T} r(t) \sin(\omega_c t + \theta) dt \right) \right) \left(\frac{2\sqrt{2S}}{N_0} \int_{kT}^{(k+1)T} r(t) \cos(\omega_c t + \theta) dt \right) \tag{lo}$$

and

$$e \triangleq \frac{d \ln v(\theta)}{d\theta} = \sum_{k=0}^{L-1} \left(\tanh\left(\frac{2\sqrt{2S}}{N_0} \int_{kT}^{(k+1)T} r(t) \sin(\omega_c t + \theta) dt \right) \right) \left(\frac{2\sqrt{2S}}{N_0} \int_{kT}^{(k+1)T} r(t) \cos(\omega_c t + \theta) dt \right) \tag{11}$$

The particular implementation of Figure 2C is what is commonly called an *I-Q MAP estimation loop [6, 7].* The special cases of Figure 2C wherein the hyperbolic tangent nonlinearity is approximated by linear and hard limiter devices, corresponding respectively to low and high signal-to-noise ratio (SNR) conditions, are commonly called the I-Q Costas loop [4] and I-Q polarity-type Costas loop [5]. For simplicity of notation, we shall refer to the three closed loop structures in Figure 2 as *AL closed loop #1, #2,* and #3.

3.2 Performance

In assessing the performance of one closed loop scheme versus another, one must be careful to normalize the loop parameters so as to allow a fair basis of comparison. In this paper, the comparison will be made on the basis of mean-squared phase error, σ_ϕ^2, *for a fixed loop bandwidth, B_L.* This is the typical measure of performance use to describe a closed loop phase synchronization structure when it is operating in its tracking mode.

An analysis of the closed loop performance of Figure 2a results in an expression for the mean-squared phase error given by[5]

‘All of the performance results given in this paper will be based upon the so-called *linear* theory [3] which assumes that the loop operates in a region of high loop SNR.

$$D_i = \sum_{k=0}^{L-1} d_k \underbrace{d_{ik} d_{ik}}_{=1} d_{ik} = \sum_{k=0}^{L-1} d_k^{'} d_{ik}^{'}$$

$$D_{ij} = \sum_{k=0}^{L-1} d_{ik} \underbrace{d_{ik} d_{ik}}_{=1} d_{jk} = \sum_{k=0}^{L-1} d_{ik}^{'} d_{jk}^{'} \tag{16}$$

where $d_k^{'} = d_k d_{ik}$ represents the kth element of some other possible transmitted sequence $\mathbf{d}' \triangleq (d_0^{'}, d_1^{'}, \ldots, d_{L-1}^{'})$ and $d_{ik}^{'} = d_{ik} d_{ik}, d_{jk}^{'} = d_{ik} d_{jk}$ are the kth elements of two other possible sequences $\mathbf{d}_i^{'} \triangleq (d_{i0}^{'}, d_{i1}^{'}, \ldots, d_{i,L-1}^{'})$ and $\mathbf{d}_j^{'} \triangleq (d_{j0}^{'}, d_{j1}^{'}, \ldots, d_{j,L-1}^{'})$, respectively. Since, in general, $\mathbf{d}' \neq$ d and since the summations on i and j in (12) range over all possible (2^L) sequences, then substitution of (16) into (12) shows that σ_ϕ^2 evaluated for a transmitted sequence equal to d' is identical to that evaluated for a transmitted sequence equal to d.

Special cases of (12) corresponding to $L = 1,2,$ and 3 are given below:

$$\sigma_\phi^2 = \frac{1}{\rho}\left[\frac{e^{8R_d R_d} - 1}{\left(e^{3R_d} - e^{-R_d}\right)^2}\right]; \qquad L=1$$

$$\sigma_\phi^2 = \frac{1}{2}\,\frac{1}{\rho}\left[\frac{e^{16R_d} + 2e^{8R_d} - 3}{\left(e^{6R_d} - \sim -\%\right)^2}\right]; \qquad L=2$$

$$\sigma_\phi^2 = \frac{1}{\rho}\left[\frac{e^{24R_d} + 5e^{16R_d} + 3e^{8R_d} - 9}{\left(e^{9R_d} + e^{5R_d} - e^{R_d} - e^{-3R_d}\right)^2}\right]; \; L = 3 \tag{17}$$

Figure 3 is a plot of S_L (in dB) 'versus R_d (in dB) corresponding to the three cases in (17). We observe that the performance of AL closed loop #1 as implemented in Figure 2c is clearly a function of the observation length of the corresponding open loop estimator that motivated the structure.

For large Rd, it is straightforward to show that σ_ϕ^2 has the asymptotic behavior

$$\sigma_\phi^2 \cong \frac{1}{\rho} e^{2LR_d} \rightarrow S_L \cong e^{-2LR_d} \tag{18}$$

For small Rd, σ_ϕ^2 has the asymptotic form

$$\sigma_\phi^2 \cong \frac{1}{\rho}\left(\frac{1}{2R_d}\right) \rightarrow \qquad S_L \cong 2R_d \tag{19}$$

which is independent of L.

Looking at (18) and Figure 3, one gets the impression (and rightfully so) that the mean-squared phase error of AL closed loop #1 becomes unbounded as R_d + *00.* This singular behavior can be traced to the fact that the $2\sqrt{2S}/N_0$ coefficient preceding the integral in the definition of $q(\theta)$ given in (4), which becomes the weighting coefficient of the two integrate-and-dump (I&D) circuits in the closed loop of Figure 2a, becomes unbounded as R_d *+00* $(N_0$ + *O).* Suppose instead that we were to replace this coefficient by an arbitrary constant, say K_0, both in the definition of $q(\theta)$ given in (4) and the closed loop motivated by this function, i.e., Figure 2a. From the standpoint of open loop estimation of θ, AL open loop estimator #1 as defined by (5) with now $2\sqrt{2S}/N_0$ replaced by K_0 would remain unchanged. That is, *the choice of the weighting constant preceding the L-bit integration has no effect on the open loop estimate.* On the other hand, the choice of this weighting coefficient for the closed loop scheme has a very definite bearing on its performance. In particular, with $2\sqrt{2S}/N_0$ replaced by K_0 in Figure 2a, the mean-squared phase error, previously given by (12) now becomes

$$\sigma_\phi^2 = \frac{1}{\rho}\left[\frac{L\sum_{i=1}^{2^L}\sum_{j=1}^{2^L} D_{ij}\exp\left\{K\left(D_i + D_j\right) + K^2\left(\frac{L}{2R_d}\right)\left(1+\frac{D_{ij}}{L}\right)\right\}}{\left[\sum_{m=0}^{L}\binom{L}{m}(L-2m)\exp\left\{K(L-2m) + K^2\left(\frac{L}{4R_d}\right)\right\}\right]^2}\right] \triangleq \frac{1}{\rho S_L} \tag{20}$$

where we have further normalized the weighting coefficient as $K \triangleq \left(\sqrt{S/2}\right)K_0 T$. Note that if we set K_0 *=2@* /NO as before, then $K = 2R_d$ and (20) reduces to (12).

From (20), we see that as long as K_0 (or equivalently K) is finite (which would be the case in a practical implementation of the AL closed loop scheme), the large SNR asymptotic behavior of AL closed loop #1 now becomes

$$\lim_{R_d\to\infty}\sigma_\phi^2 = \lim_{N_0\to 0}\frac{N_0 B_L}{S}\left[\frac{L\sum_{i=1}^{2^L}\sum_{j=1}^{2^L} D_{ij}\exp\left\{K\left(D_i + D_j\right)\right\}}{\left[\sum_{m=0}^{L}\binom{L}{m}(L-2m)\exp\{K(L-2m)\}\right]^2}\right] = 0 \tag{21}$$

which is what one would expect. What is interesting is that, for any value of R_d, the value of K that minimizes (20), which, from the standpoint of *closed* loop performance as measured by mean-squared phase error, would be considered optimum is $K \to O$, *independent* of *Rd.* In fact, if one takes the limit of (20) as K + O (this must be done carefully using the properties in Table), the following result is obtained:

$$\lim_{K\to 0}\sigma_\phi^2 \triangleq \left(\sigma_\phi^2\right)_{\min} = \frac{1}{\rho}\left[1+\frac{1}{2R_d}\right] \quad \rightarrow \quad \left(\mathcal{S}_L\right)_{\max} = \frac{1}{1+\frac{1}{2R_d}} = \frac{2R_d}{1+2R_d} \tag{22}$$

Interestingly enough, the result in (22), *which* is *now* independent *of L, is* also characteristic of the performance of the I-Q Costas loop [4] which is obtained as a low SNR approximation to AL closed loop #3. It is important to understand that the optimum closed loop performance of (22) results as a consequence of optimizing the weight (gain) K for each value of L. If instead of doing this one were to fix the gain K for all values of L (as suggested by the MAP estimation approach), then the closed loop performance (as measured by σ_ϕ^2 with fixed loop bandwidth) is suboptimum and indeed depends once again on L. One final note is to point out that the small SNR behavior of (22) is identical to (19) the reason being that the value of $K = 2R_d$ used in arriving at (19) approaches the optimum value (K = O) as $R_d \rightarrow O$.

The performance of AL closed loop #2 is difficult to obtain in closed form. Thus, because of its unorthodox structure, we shall not pursue it in this paper. Instead we move on to AL closed loop #3 whose performance has been obtained previously [6]. In particular, the mean-squared phase error performance of this loop is given by

$$\sigma_\phi^2 = \frac{1}{\rho}\left[\frac{\overline{\tanh^2\left\{2R_d-\sqrt{2R_d}X\right\}}}{\left[\overline{\tanh\left\{2R_d-\sqrt{2R_d}X\right\}}\right]^2}\right] \triangleq \frac{1}{\rho\mathcal{S}_L} \tag{23}$$

where X is a zero mean, unit variance Gaussian random variable and the overbar denotes statistical averaging over X. A plot of S' versus Rd is superimposed on the curves of Figure 3. We first note that the performance as given by (23) is independent of L. Furthermore, a comparison of the squaring loss as determined from (23) with that calculated from (22) reveals that the performance of AL closed loop #3 is superior to that of AL closed loop #1 with optimized gain for all values of Rd (see Figure 3 of [6]). As mentioned previously, if the hyperbolic tangent nonlinearity in Figure 2c is approximated by a linear device (i.e., $\tanh x \cong x$), then the two loops have the same performance.

What is particularly interesting for AL closed loop #3 is that even though the performance in (23) is computed assuming a weighting coefficient in front of the I&D's in Figure 2C equal to 2=/ NO , the behavior of this loop is not singular in the limit as

$R_d \to \infty$. Furthermore, it is natural to ask whether the above weighting coefficient is indeed optimum in the sense of minimizing σ_ϕ^2. To answer this question we proceed as was done for AL closed loop #1, namely, we replace the weighting coefficient $2\sqrt{2S}/N_0$ in (6) by an arbitrary constant, say K_0, (hence the same replacement is made in the corresponding closed loop error signal of (11)) and proceed to optimize the performance with respect to the choice of this gain.[7] Making this replacement produces a mean-squared phase error, analogous to (23), given by

$$\sigma_\phi^2 = \frac{1}{\rho}\left[\frac{\overline{\tanh^2\left\{K\left[2R_d - \sqrt{2R_d}X\right]\right\}}}{\left[\overline{\tanh\left\{K\left[2R_d - \sqrt{2R_d}X\right]\right\}}\right]^2}\right] \triangleq \frac{1}{\rho S_L} \tag{24}$$

where, as before, we have further normalized the weighting coefficient as $K \triangleq K_0 N_0 / 2\sqrt{2S}$. Maximizing the squaring loss factor S_L (i.e., minimizing σ_ϕ^2) in (24) results in $K = 1$ *(K. =2@ / NO) for all values of Rd.* Thus, for AL closed loop #3, *the optimum gain from the standpoint of closed loop performance is precisely that dictated by the open loop MAP estimation* of θ and the best performance is that described by (23).

We conclude our discussion of AL closed loops by pointing out that, in view of the superiority of (23) over (22), AL closed loop #3 outperforms AL closed loop #1 for all values of Rd.

4.0 Closed LooPs Motivated bv the ML Approach

4.1 Structures

The ML approach to estimating the carrier phase, θ, is to maximize (rather than average) $p(r(t)\,d_i(t),\theta)$ over all possible (2^L) and equally likely data sequences yielding the conditional pdf

$$\begin{aligned} p(r(t)|\theta) &= \max_{\{d_i(t)\}} p(r(t)|d_i(t),\theta) = \max_{\{d_i(t)\}} \exp\left(\frac{2\sqrt{2S}}{N_0}\int_0^{LT} r(t)d_i(t)\sin(\omega_c t + \theta)dt\right) \\ &= \exp\left(\max_{\{d_i(t)\}}\frac{2\sqrt{2S}}{N_0}\int_0^{LT} r(t)d_i(t)\sin(\omega_c t + \theta)dt\right) \triangleq q_{\hat{i}}(\theta) \end{aligned} \tag{25}$$

where $\hat{i}$ is the particular value of i corresponding to the data waveform $d_{\hat{i}}(t)$ that achieves the maximization in (25). Analogous to (5), *ML* open loop *estimator #1 is* obtained by finding the value of θ that maximizes $q_{\hat{i}}(\theta)$ of (25), i.e.,

[7] Again we note that this replacement does not effect the open loop estimation of O using (6).

$$\hat{\theta} = \max_{\theta}{}^{-1} q_i(\theta) \tag{26}$$

A block diagram implementation of this estimator is illustrated in Figure 4a.

Alternately, breaking up the integration over the entire observation into a sum of integrals on each bit interval and recognizing that the data bits are iid binary random variables, then (25) together with (26) evaluates to

$$\begin{aligned}\hat{\theta} &= \max_{\theta}{}^{-1} \max_{\{d_k\}} \prod_{k=0}^{L-1} \exp\left(\frac{2\sqrt{2S}}{N_0} \int_{kT}^{(k+1)T} r(t) d_k \sin(\omega_c t + \theta) dt \right) \\ &= \max_{\theta}{}^{-1} \prod_{k=0}^{L-1} \max_{\{d_k\}} \exp\left(\frac{2\sqrt{2S}}{N_0} \int_{kT}^{(k+1)T} r(t) d_k \sin(\omega_c t + \theta) dt \right) \\ &= \max_{\theta}{}^{-1} \prod_{k=0}^{L-1} \exp\left(\left| \frac{2\sqrt{2S}}{N_0} \int_{kT}^{(k+1)T} r(t) \sin(\omega_c t + \theta) dt \right| \right)\end{aligned} \tag{27}$$

This estimator is analogous to (7) and is called *ML open loop estimator #2*. A block diagram implementation of this estimator is illustrated in Figure 4b.

Next, we obtain ML open loop estimates by maximizing the natural logarithm of $q_i(\theta)$. Using the product form of $q_i(\theta)$ as in (27), one obtains

$$\begin{aligned}\hat{\theta} &= \max_{\theta}{}^{-1} \ln \max_{\{d_k\}} \prod_{k=0}^{L-1} \exp\left(\frac{2\sqrt{2S}}{N_0} \int_{kT}^{(k+1)T} r(t) d_k \sin(\omega_c t + \theta) dt \right) \\ &= \max_{\theta}{}^{-1} \ln \prod_{k=0}^{L-1} \max_{\{d_k\}} \exp\left(\frac{2\sqrt{2S}}{N_0} \int_{kT}^{(k+1)T} r(t) d_k \sin(\omega_c t + \theta) dt \right) \\ &= \max_{\theta}{}^{-1} \ln \prod_{k=0}^{L-1} \exp\left(\left| \frac{2\sqrt{2S}}{N_0} \int_{kT}^{(k+1)T} r(t) \sin(\omega_c t + \theta) dt \right| \right) \\ &= \max_{\theta}{}^{-1} \sum_{k=0} \left| \frac{2\sqrt{2S}}{N_0} \int_{kT}^{(k+1)T} r(t) \sin(\omega_c t + \theta) dt \right|\end{aligned} \tag{28}$$

which is analogous to (8) and therefore called *ML open loop estimator #3*. Its block diagram implementation is illustrated in Figure 4c.

Finally, we consider a fourth ML open loop estimator which is based on maximizing the natural logarithm of $q_i(\theta)$ in its unpartitioned form of (25). This leads to *ML open loop estimator #4* which is defined by

$$\hat{\theta} = \max_{\theta}^{-1} \ln q_{\hat{i}}(\theta) = \max_{\theta}^{-1} v_{\hat{i}}(\theta) = \max_{\theta}^{-1} \frac{2\sqrt{2S}}{N_0}\int_0^{LT} r(t)d_{\hat{i}}(t)\sin\left(\omega_c t + \theta\right)dt \qquad (29)$$

and illustrated in Figure 4d. Recognizing that the exponential function in Figure 4d can be eliminated, we get the alternate and simpler form of Figure 4e. Although an analogous AL open estimator could have been derived from in $q(\theta)$ with $q(\theta)$ defined in (4), we chose not to do so since there is no apparent advantage gained by taking the natural logarithm of a *sum* of exponentials.

As was true for the AL case, it is important to emphasize that the four ML open loop phase estimates as described by (26) - (29) are identical. Thus, from the standpoint of finding the optimum open loop phase estimate, it makes no difference which of the four structures in Figure 4 is implemented, i.e., they all yield the same performance. Again we shall see that this same statement is *not* true when considering the performances of the closed loops motivated by these four different ML formulations.

A closed loop phase synchronization structure based on ML open loop estimator #1 is illustrated in Figure 5a where, in accordance with the discussion given in the introduction, the error signal, e, is given by [see Eq. (26)]

$$e \triangleq \frac{dq_{\hat{i}}(\theta)}{d\theta} = \exp\left(\frac{2\sqrt{2S}}{N_0}\int_0^{LT} r(t)d_{\hat{i}}(t)\sin\left(\omega_c t + \theta\right)dt\right) \times \frac{2\sqrt{2S}}{N_0}\int_0^{LT} r(t)d_{\hat{i}}(t)\cos\left(\omega_c t + \theta\right)dt \qquad (30)$$

Analogous closed loop phase synchronization structures corresponding to ML open loop estimators #2, #3, and #4 are illustrated in Figure 5b, c, and d where the error signals are respectively given by [see (27) - (29)]

$$e = \prod_{k=0}^{L-1} \exp\left(\left|\frac{2\sqrt{2S}}{N_0}\int_{kT}^{(k+1)T} r(t)\sin\left(\omega_c t + \theta\right)dt\right|\right) \times \sum_{k=0}^{L-1} \frac{2\sqrt{2S}}{N_0}\int_{kT}^{(k+1)T} r(t)d_{\hat{k}}\cos\left(\omega_c t + \theta\right)dt$$

$$d_{\hat{k}} = \operatorname{sgn}\left\{\frac{2\sqrt{2S}}{N_0}\int_{kT}^{(k+1)T} r(t)\sin\left(\omega_c t + \theta\right)dt\right\} \qquad (31)$$

$$e = \sum_{k=0}^{L-1} \frac{2\sqrt{2S}}{N_0}\int_{kT}^{(k+1)T} r(t)d_{\hat{k}}\cos\left(\omega_c t + \theta\right)dt \qquad (32)$$

$$e = \frac{2\sqrt{2S}}{N_0}\int_0^{LT} r(t)d_{\hat{i}}(t)\cos\left(\omega_c t + \theta\right)dt \qquad (33)$$

Analogous to the terminology used for the AL case, we shall refer to the four closed loop structures in Figure 5 as *ML closed loop #1, #2, #3, and #4.* It is worthy of note that ML closed loop #3 is identical in form to the I-Q polarity-type Costas loop [5].[8] We recall that, in the AL case, the I-Q polarity-type Costas loop is obtained only as a high SNR approximation to closed loop #3.

4.2 Performance

An analysis of the closed loop performance of Figure 5a results in an expression for the mean-squared phase error given by (see Appendix A for the derivation)

$$\sigma_\phi^2 = \frac{1}{\rho}\left[\frac{L^2\sum_{m=0}^{L} P_0(m)\exp\{8R_d(L-m)\}}{\left[\sum_{m=0}^{L} P_0(m)(L-2m)\exp\{R_d(3L-4m)\}\right]^2}\right] \triangleq \frac{1}{\rho S_L}$$

$$P_0(m) = \binom{L}{m} p_0^m (1-p_0)^{L-m}, \quad p_0 = \frac{1}{2}\operatorname{erfc}\sqrt{R_d} \tag{34}$$

As was true for the analogous AL closed loop (see Figure 3), the mean-squared phase error of ML closed loop #1 as given by (34) becomes unbounded as $R_d \to \infty$. This singular behavior can again be remedied by replacing the $2\sqrt{2S}/N_0$ coefficient in front of the I&D's in Figure 5a by an arbitrary constant, say K_0 which remains finite as $N_0 \to 0$. With this replacement, the mean-squared phase error now becomes

$$\sigma_\phi^2 = \frac{1}{\rho}\left[\frac{L^2\sum_{m=0}^{L} P_0(m)\exp\left\{2K(L-2m) + K^2\left(\frac{L}{R_d}\right)\right\}}{\left[\sum_{m=0}^{L} P_0(m)(L-2m)\exp\left\{K(L-2m) + K^2\left(\frac{L}{4R_d}\right)\right\}\right]^2}\right] \triangleq \frac{1}{\rho S_L} \tag{35}$$

where, as before, we have further normalized the weighting coefficient as $K \triangleq \left(\sqrt{S/2}\right)K_0 T$. As long as K_0 (or equivalently K) is finite (which would be the case in a practical implementation of the ML closed loop scheme), the large SNR asymptotic behavior of ML closed loop #1 is

[8]The L-fold accumulator that precedes the loop filter can be absorbed into the loop filter itself by renormalizing its bandwidth. Thus, when making comparisons with analogous configurations, this accumulator can be omitted,

$$\lim_{R_d \to \infty} \sigma_\phi^2 = \lim_{N_0 \to 0} \frac{N_0 B_L}{S} \left| \frac{L' \sum_{m=0}^{L} P_0(m) \exp\{[2K(L-2m)]\}}{\left[\sum_{m=0}^{L} P_0(m)(L-2m)\exp\{[K(L-2m)]\}\right]^2} \right| = 0 \qquad (36)$$

as one would expect. What is indeed interesting is that, *unlike* the AL case, the value of K that minimizes (35), which from the standpoint of *closed* loop performance as measured by mean-squared phase error would be considered optimum, is ***not*** $K \to$ O, In fact, for each value of Rd and L, there exists an optimum value of K *which* unfortunately cannot be determined in closed form. Nevertheless, the optimum values of K can be found numerically as a function of Rd by maximizing $\mathcal{S}_L$ as determined from (35) for each value of L. The results are illustrated in Figure 6. The corresponding values of $(\mathcal{S}_L)_{max}$ are plotted versus R_d in dB in Figure 7 for the same values of L as in Figure 6. Also illustrated in Figure 7 is the value of $\mathcal{S}_L$ corresponding to K + O which is determined from (35) as

$$\lim_{K \to 0} \sigma_\phi^2 = \left(\sigma_\phi^2\right)_0 = \frac{1}{\rho}(1-2p)^{-2} = \frac{1}{\rho}\left(\operatorname{erf}^2 \sqrt{R_d}\right)^{-1} \qquad + \left(\mathcal{S}_L\right)_0 = \operatorname{erf}^2 \sqrt{R_d} \qquad (37)$$

and which is ***independent of the** observation **length*** L. Since the optimum value of K is always greater than zero (see Figure 6), then (37) serves as a lower bound on the squaring loss performance of ML closed loop #1. Other reasons for including this limiting squaring loss behavior in Figure 7 will become apparent shortly when we consider the other ML closed loop configurations.

From Figure 7 we observe that the performance of ML closed loop #1 becomes worse with increasing *L, i.e., L* = 1 gives the best performance. Also in the limit as *L + 00,* the optimum value of K approaches zero independent of R_d. Thus, the limiting performance for *L +00 is* also given by (37).

As in the AL case, the performance of ML closed loop #2 is difficult to obtain in closed form and because of its unorthodox structure we shall not pursue it in this paper. Moving on to ML closed loop *#3, we* previously identified this as being identical in form to the I-Q polarity-type Costas loop. Hence, its performance is independent of L and is given by (37). Furthermore, it is straightforward to show that the performance of ML closed loop #4 is also independent of L and given by (37). Thus, we see that of the three ML closed loops (#1, #3, #4) whose performance has been evaluated, ML closed loop #1 is superior to the other two which have performances that are identical and equal to that of the former in the worst case *($L \to$ 00).*

Perhaps the most interesting result of all of what has been discussed thus far is obtained when the performance of the best ML closed scheme (i.e., #1) is compared with that of the best AL scheme (i.e., #3), the I-Q MAP estimation loop which heretofore has stood as the pillar of performance among BPSK tracking loops. This comparison is illustrated in Figure 8 where the squaring loss is plotted versus R_d for the two schemes. We observe that for small values of R_d , as is encountered in systems employing a combination of low rate codes [1 O] and antenna arraying [11], *ML closed loop #1 outperforms the I-Q MAP estimation loop which itself outperforms the well-known I-Q Costas loop and I-Q polarity-type Costas loop.*

4.3 Loop S-Curves

It is of interest to examine the S-curve behavior of ML closed loop #1 and compare it with that of ML closed loop #3 and AL closed loop #3. The equation describing the loop S-curve, $\eta(\phi)$, of ML closed loop #1 is derived in Appendix A as Eq. (A-9) with the special case of $L = 1$ (already shown to yield the best tracking performance) given by Eq. (A-1 O). Figure 9 illustrates plots of $\eta(\phi)$ versus ϕ over one cycle of π radians for R_d = -5, 0, and 5 dB, respectively, where in each case, K has been chosen equal to the optimum value as determined from Figure 6. In the limit of small and large Rd, the S-curve approaches the following functional forms:

$$\eta(\phi) \propto \begin{cases} \sin 2\phi, & \text{small } R_d \\ \sin\phi \times \operatorname{sgn}(\cos\phi), & \text{large } R_d \end{cases} \qquad (38)$$

These limiting forms are identical to the same limiting behavior of the S-curves corresponding to ML closed loop #3 – the I-Q polarity-type Costas loop, and AL closed loop #3 – the I-Q MAP estimation loop.

5.0 Conclusions

Motivated by the theory of MAP carrier phase estimation, we have developed a number of closed loop structures suitably derived from maximum-likelihood (ML) and average-likelihood (AL) functions. Several of these structures reduce to previously known closed loop carrier phase synchronizers while others appear to be new. Of particular interest is one of the ML structures which, when properly optimized, gives improved mean-square phase error performance over the other ML and AL structures. The improvement is largest at low symbol SNR and is thus quite significant in applications that involve a combination of low rate coding and antenna arraying such as the NASA/JPL Galileo mission to Jupiter [10, 11]. We leave the reader with the thought that the structures proposed in this paper are not exhaustive of the ways that closed loop phase synchronizers can be derived from open loop MAP estimation theory. Rather they are given here primarily to indicate the variety of different closed loop schemes that can be constructed simply from likelihood and log-likelihood functions.

Acknowledgment

The authors would like to thank Prof. Bruce Hajek of the University of Illinois for his constructive comments during the course of the development.

References

[1] Helstrom, C. W., Statistical *Theory of Signal Detection,* Pergamon Press (Macmillan Co.), New York, NY, 1960.

[2] VanTrees, H. L., *Detection Estimation, and Modulation Theory, Part I,* John Wiley & Sons, New York, NY, 1968.

[3] Stiffler, J. J. *Theory* Of *Synchronous Communications,* Prentice Hall, Inc., Englewood Cliffs, NJ, 1971.

[4] Lindsey, W.C. and Simon, M. K., "Optimum Design ad Performance of Suppressed Carrier Receivers with Costas Loop Tracking," IEEE Transactions on Communications, Vol. COM-25, No. 2, February 1977, pp. 215-227.

[5] Simon, M. K., "Tracking Performance of Costas Loops with Hard Limited In-Phase Channel," IEEE Transactions on Communications, Vol. COM-26, No. 4, April 1978, pp. 420-432.

[6] Simon, M. K., "On the Optimality of the MAP Estimation Loop for Tracking BPSK and QPSK Signals, " IEEE Transactions on Communications, Vol. COM-27, No. 1, January 1979, pp. 158-165.

[7] Simon, M. K., "Optimum Receiver Structures for Phase-Multiplexed Modulations," IEEE Transactions on Communications, Vol. COM-26, No. 6, June *1978,* pp. 865-872,

[81 Simon, M. K., "On the Calculation of Squaring Loss in Costas Loops with Arbitrary Arm Filters," IEEE Transactions on Communications, Vol. COM-26, No. 1, January 1978, pp. 179-184.

[9] Simon, M. K. and Alem, W. K., "Tracking Performance of Unbalanced QPSK Demodulators' Part II - Biphase Costas Loop with Active Arm Filters," IEEE Transactions on Communications, Vol. COM-26, No. 8, August 1978, pp. 1157-1166.

[10] Dolinar, S., "A New Code for Galileo," TDA Progress Report 42-93, January-March 1988, Jet Propulsion Laboratory, Pasadena, CA, pp. 83-96.

[11] Mileant, A. and Hinedi, S., "Overview of Arraying Techniques for Deep Space Communications," accepted for publication in the IEEE Transactions on Communications.

Appendix A

Derivation of the Closed Loop Tracking Performance of ML Closed Loop #1

Consider the closed loop in Figure 5a whose error signal, $e(t)$, at time t = LT is characterized by Eq. (30) with $2\sqrt{2S}\ /\ N_0$ replaced by K_0, that is

$$e = \exp\left(K_0 \int_0^{LT} r(t) d_i(t) \sin(\omega_c t + \theta) dt\right) \times K_0 \int_0^{LT} r(t) d_i(t) \cos(\omega_c t + \theta) dt \tag{A-1}$$

Substituting r(t) of (1) into (30) results in

$$e = \exp\left\{K_0\sqrt{\frac{S}{2}}\left(\int_0^{LT} d(t) d_i(t) dt\right)\cos\phi + \underbrace{K_0 \int_0^{LT} n(t) d_i(t) \sin(\omega_c t + \theta) dt}_{n_s'}\right\}$$

$$\times\left[K_0\sqrt{\frac{S}{2}}\left(\int_0^{LT} d(t) d_i(t) dt\right)\sin\phi + \underbrace{K_0 \int_0^{LT} n(t) d_i(t) \cos(\omega_c t + \theta) dt}_{n_c'}\right] \tag{A-2}$$

where n_s' and n_c' are zero mean Gaussian random variables with variance $\sigma^2_{n_s'} = \sigma^2_{n_c'} = K_0^2 LTN_0\ /\ 4$. In view of the rectangular pulse shape assumed for the transmitted data waveform, d (t), in (2), the correlation $\int_0^{LT} d(t) d_i(t) dt$ in (A-2) can be expressed in terms of the cross-correlation $D_i = \sum_{k=0}^{L-1} d_k d_{ik}$ defined in (14) by

$$\int_0^{LT} d(t) d_i(t) dt = TD_i \tag{A-3}$$

Substituting (A-3) in (A-2) and normalizing n_s' and n_c' to unit variance Gaussian random variables, N, and N_c, respectively, we get[1]

$$e = \exp\left\{K_0\sqrt{\frac{S}{2}} TD\cos\phi + K_0\sqrt{\frac{LTN_0}{4}} N_s\right\} \times \left(K_0\sqrt{\frac{S}{2}} TD\sin\phi + K_0\sqrt{\frac{LTN_0}{4}} N_c\right) \tag{A-4}$$

Introducing the further normalization $K = K_0 T\sqrt{S/2}$ (note that when K_0 =2@/ No,

---

[1] For simplicity of notation, we shall drop the $\hat{i}$ subscript on D since all that is needed in what follows is the fact that D is a binomially distributed random variable which takes on values $(L\text{-}2m), m = o,$ 1,2, ... L with probability P(m)= $\binom{L}{m} p^m (1 - p)^{L-m}$, $p = \frac{1}{2}\operatorname{erfc}\left(\sqrt{R_d}\cos\phi\right)$.

i.e., the gain suggested by the open loop MAP estimation theory, then $K = 2R_d$), (A-4) becomes

$$e = \exp\left\{KD\cos\phi + K\sqrt{\frac{L}{2R_d}}N_s\right\}\times\left(KD\sin\phi + K\sqrt{\frac{L}{2R_d}}N_c\right) \quad \text{(A-5)}$$

Let $\eta(\phi)$ denote the signal component (mean) of the error sample e. Then, because of the independence of N_S and N_C, we have

$$\eta(\phi) = K\sin\phi\left(\overline{D\exp\left\{KD\cos\phi + K\sqrt{\frac{L}{2R_d}}N_s\right\}}^{D,N_s}\right) \quad \text{(A-6)}$$

where the overbar denotes statistical averaging over D and N_S. Performing first the statistical average over N_S gives

$$\overline{\exp\left\{K\sqrt{\frac{L}{2R_d}}N_s\right\}}^{N_s} = \exp\left\{K^2\frac{L}{4R_d}\right\} \quad \text{(A-7)}$$

Thus, (A-6) simplifies to

$$\eta(\phi) = K\sin\phi\left(\overline{D\exp\{KD\cos\phi\}}^{D}\right)\exp\left\{K^2\frac{L}{4R_d}\right\} \quad \text{(A-8)}$$

Finally, averaging over the binomially-distributed D, we get

$$\eta(\phi) = K\sin\phi\sum_{m=0}^{L}P(m)(L-2m)\exp\left\{K(L-2m)\cos\phi + K^2\frac{L}{4R_d}\right\} \quad \text{(A-9)}$$

which represents the S-curve of the loop. As an example, for $L = 1$, (A-9) evaluates to

$$\eta(\phi) = 2K\exp\left(\frac{K^2}{4R_d}\right)\sin\phi\left[(1-p)\exp(K\cos\phi) - p\exp(-K\cos\phi)\right] \quad \text{(A-10)}$$

which, using the definition of p, is periodic in ϕ with period π.

The slope of the S-curve at $\phi = 0$ is need for computing the closed loop mean-squared phase error performance. Differentiating (A-10) with respect to ϕ and evaluating the result at $\phi = 0$ gives

$$K_\eta \triangleq \frac{d\eta(\phi)}{d\phi}\bigg|_{\phi=0} = K\sum_{m=0}^{L}P_0(m)(L-2m)\exp\left\{K(L-2m) + K^2\frac{L}{4R_d}\right\} \quad \text{(A-11)}$$

where $P_0(m)$ is the binomial pdf of D evaluated at $\phi = 0$, namely,

$$PO(m) = \binom{L}{m} p_0^m (1-p_0)^{L-m}, \quad P. = \frac{1}{2}\operatorname{erfc}\sqrt{R_d} \tag{A-12}$$

The noise component of e evaluated at ϕ = O is

$$N = \exp\left\{KD + K\sqrt{\frac{L}{2R_d}}N_s\right\} \times \left(K\sqrt{\frac{L}{2R_d}}N_c\right) \tag{A-13}$$

which is zero mean and has variance

$$\sigma_N^2 = K^2\left(\frac{L}{2R_d}\right)\overline{\left\{\exp\left[2KD + 2K\sqrt{\frac{L}{2R_d}}N_s\right]\right\}}^{D,N_s} \tag{A-14}$$

Using (A-7) to evaluate the average over N_S, we get

$$\sigma_N^2 = K^2\left(\frac{L}{2R_d}\right)\overline{\exp\left(2K\sqrt{\frac{L}{2R_d}}N_s\right)}^{N_s}\ \overline{\exp(2KD)}^{D}$$

$$= K^2\left(\frac{L}{2R_d}\right)\sum_{m=0}^{L} P_0(m)\exp\left\{2K(L-2m) + K^2\frac{L}{R_d}\right\} \tag{A-15}$$

Since e(f) is a piecewise constant (over intervals of length LT) random process with independent increments, its statistical autocorrelation function is triangular ' and given by

$$R_e(\tau) \triangleq \left\langle E\{e(t)e(t+\tau)\}\right\rangle = \begin{cases}\sigma_N^2, & |\tau| \le LT \\ 0, & \text{otherwise}\end{cases} \tag{A-16}$$

where $\langle\bullet\rangle$ denotes time averaging which is necessary because of the cyclostationarity of $e(t)$. As is customary in analyses of this type, we assume a narrowband loop, i.e., a loop bandwidth B_L ccl/T. Then, $e(t)$ is approximated as a delta-correlated process with effective power spectral density

$$\frac{N_0'}{2} \triangleq \int_{-\infty}^{\infty} R_e(\tau)d\tau = LT\sigma_N^2 \tag{A-17}$$

Finally, the mean-squared phase error for the closed loop is

$$\sigma_\phi^2 = \frac{N_0' B_L}{K_\eta^2} \tag{A-18}$$

which upon substitution of (A-11) and (A-17) results in Eq. (35) of the main text.

Table I

Useful Properties of the Correlations D_i and D_{ij}

$$\sum_{i=1}^{2^L}\sum_{j=1}^{2^L} D_{ij} = 0$$

$$\sum_{i=1}^{2^L}\sum_{j=1}^{2^L} D_i D_{ij} = \sum_{i=1}^{2^L}\sum_{j=1}^{2^L} D_j D_{ij} = 0$$

$$\sum_{i=1}^{2^L}\sum_{j=1}^{2^L} D_{ij}^2 = 2^L \sum_{m=0}^{L} \binom{L}{m} (L-2m)^2 = 2^{2L} L$$

$$\sum_{i=1}^{2^L}\sum_{j=1}^{2^L} D_i D_j D_{ij} = 2^{2L} L$$

a) AL Open Loop Estimator #1

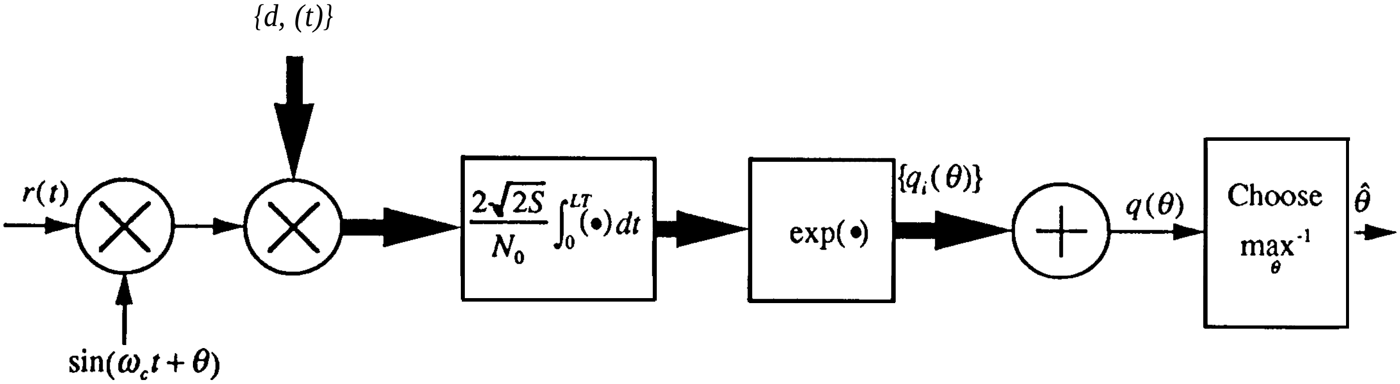

b) AL Open Loop Estimator #2

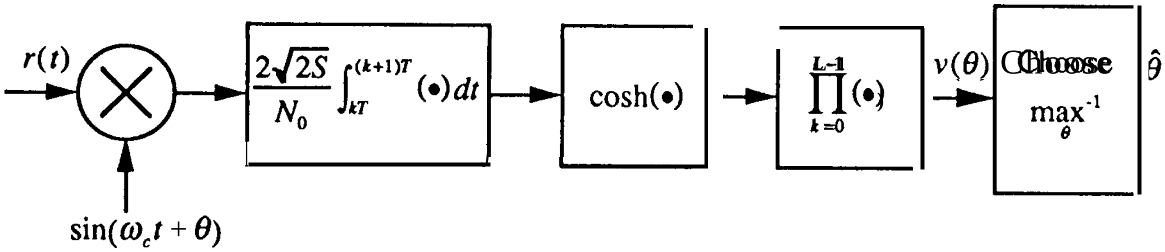

c) AL Open Loop Estimator #3

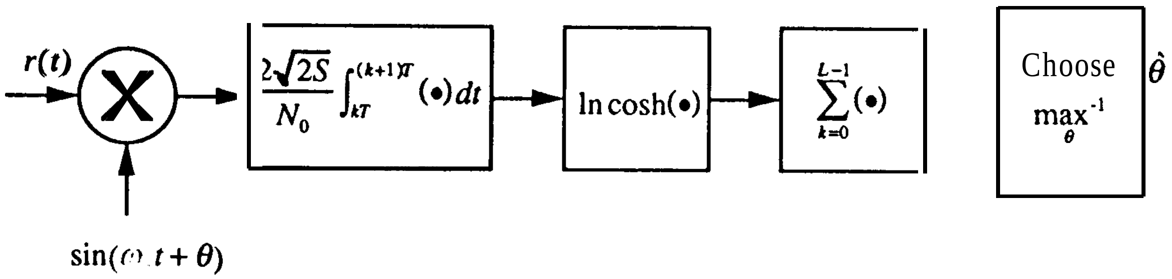

Figure 1. Three AL Open Loop Carrier Phase Estimators

a) AL Closed Loop #1

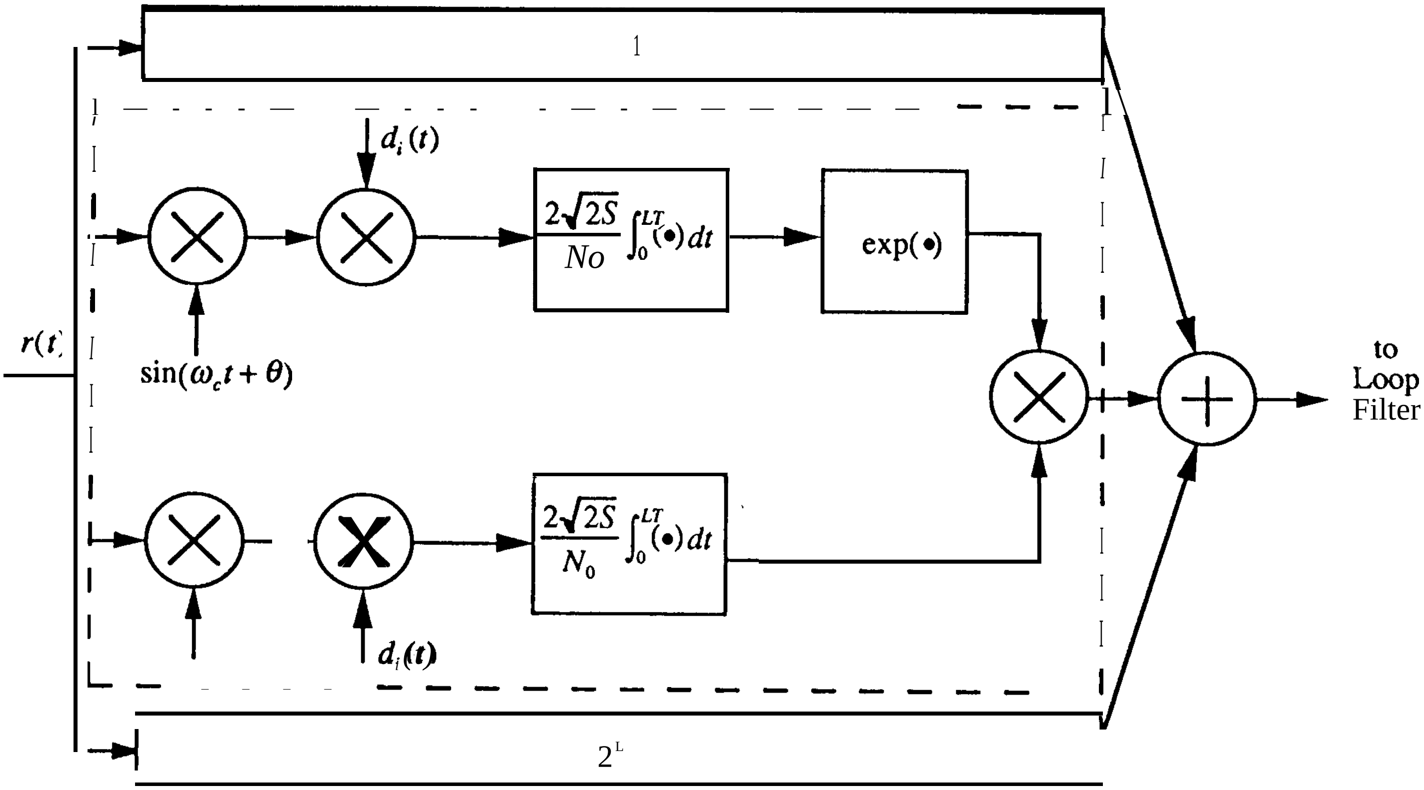

b) AL Closed Loop #2

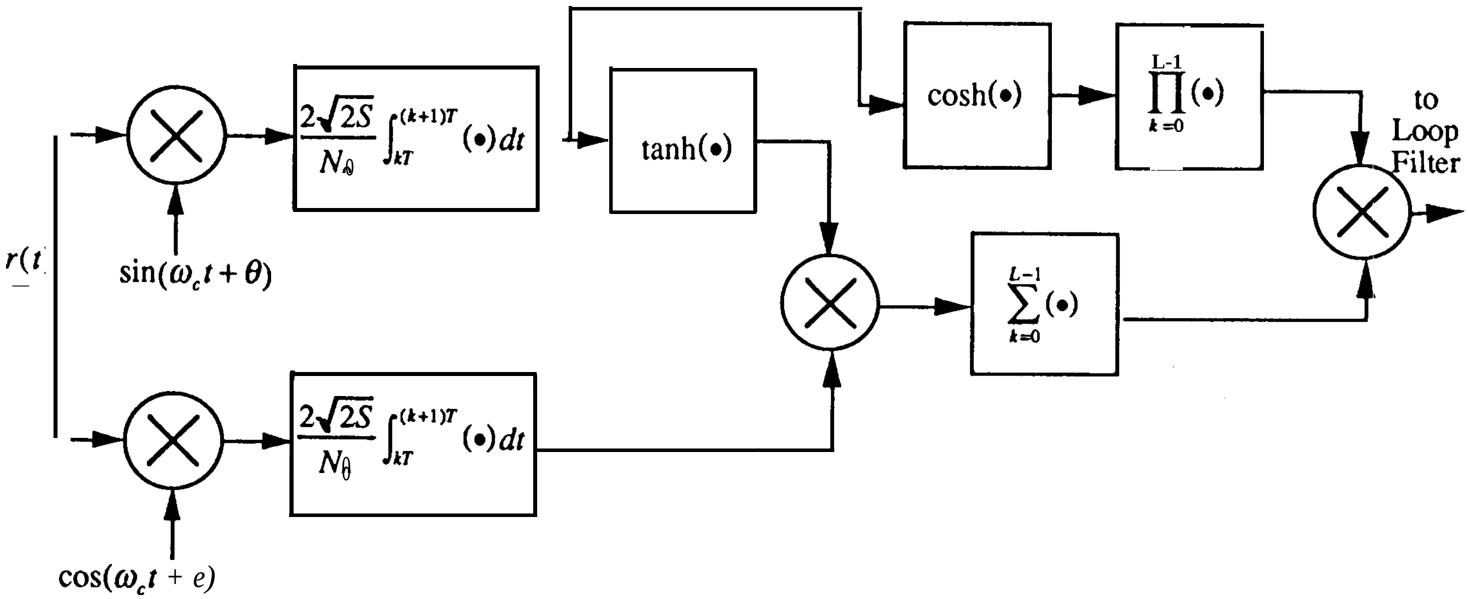

Figure 2. Three AL Closed Loop Carrier Phase Tracking Schemes

c) AL Closed Loop #3

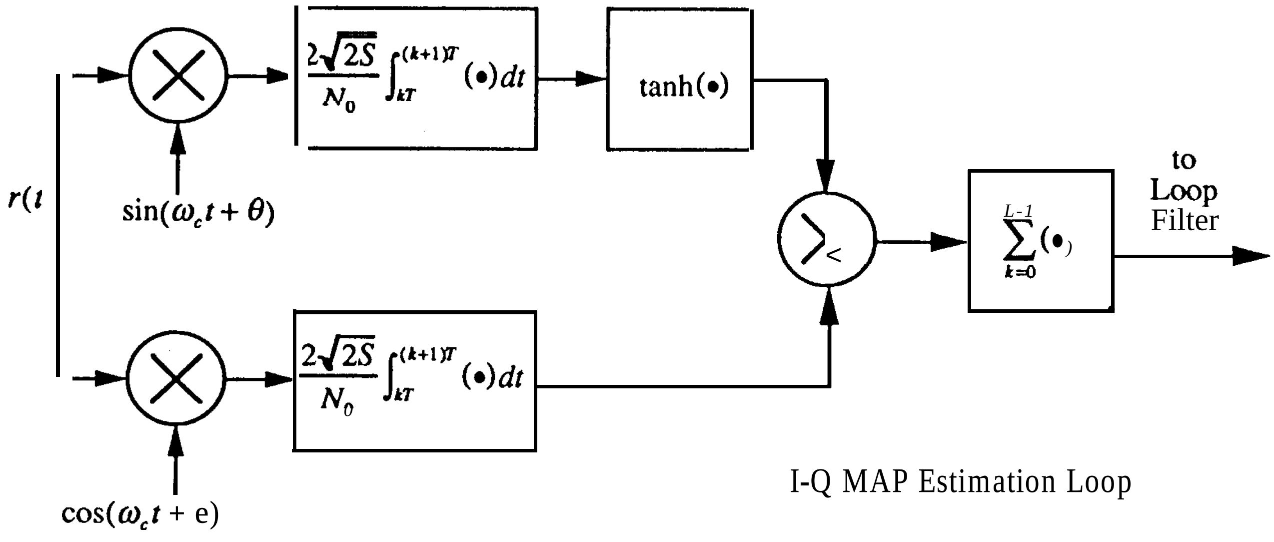

I-Q MAP Estimation Loop

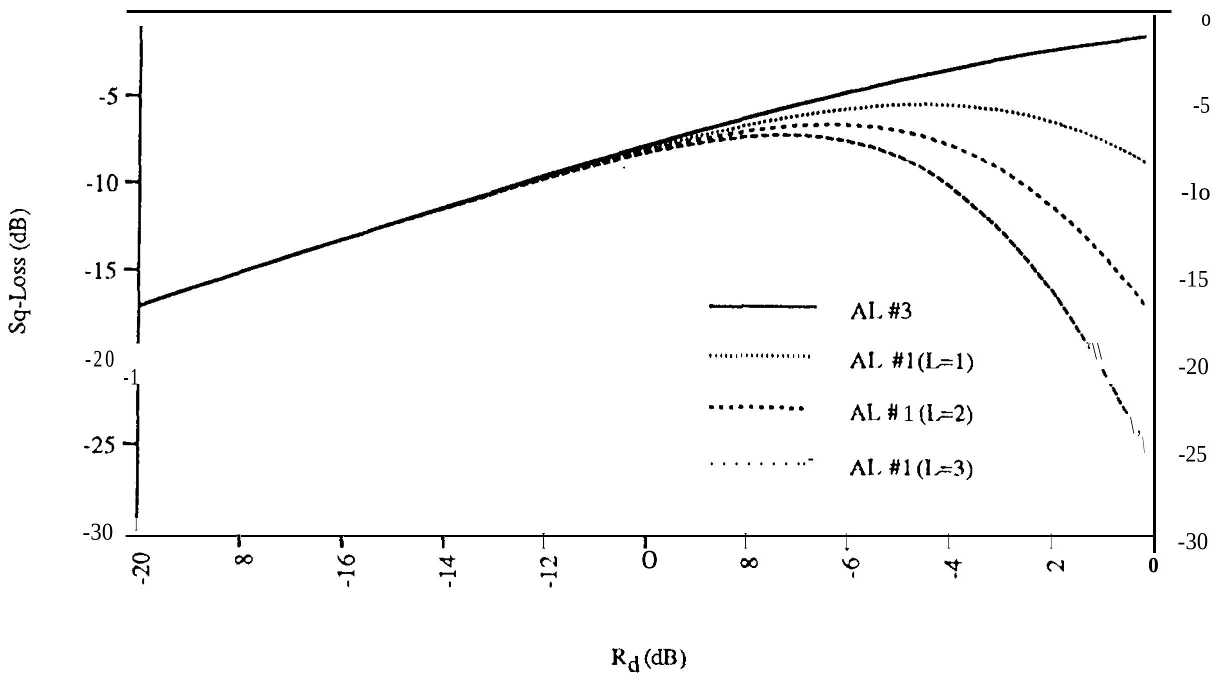

Figure 3. Squaring Loss Performance of AL Closed Loop #1 with Observation Length L as a Parameter - I&D Weighting Coefficients as Determined by MAP Estimation Theory

a) ML Open Loop Estimator # 1

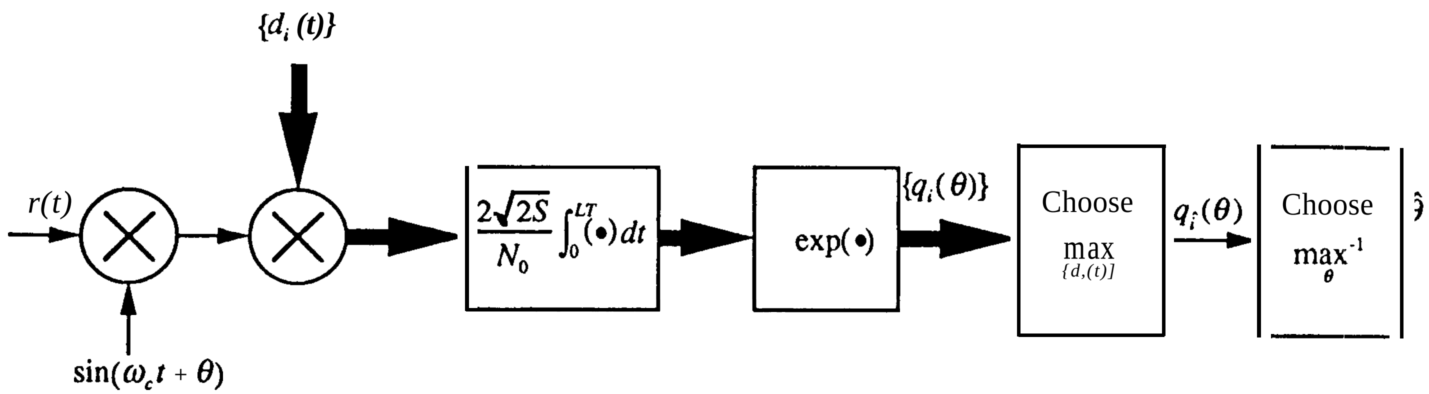

b) ML Open Loop Estimator #2

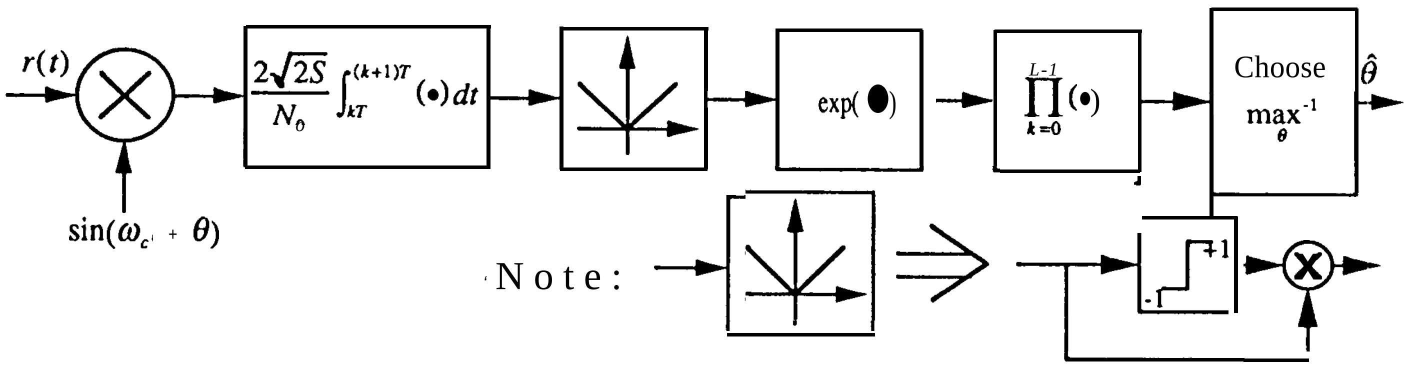

Figure 4. Four ML Open Loop Carrier Phase Estimators

c) ML Open Loop Estimator #3

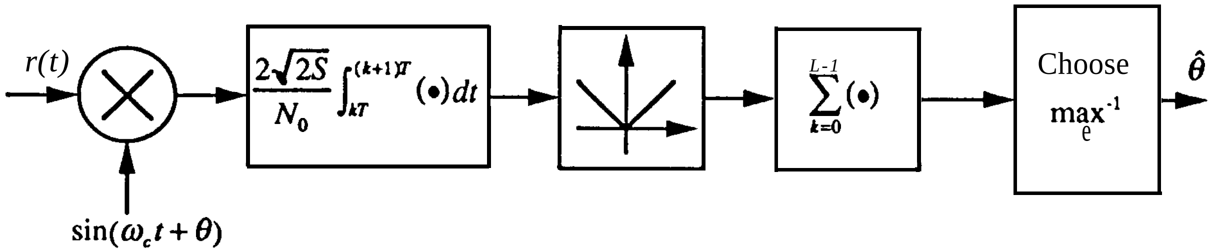

d) ML Open Loop Estimator #4

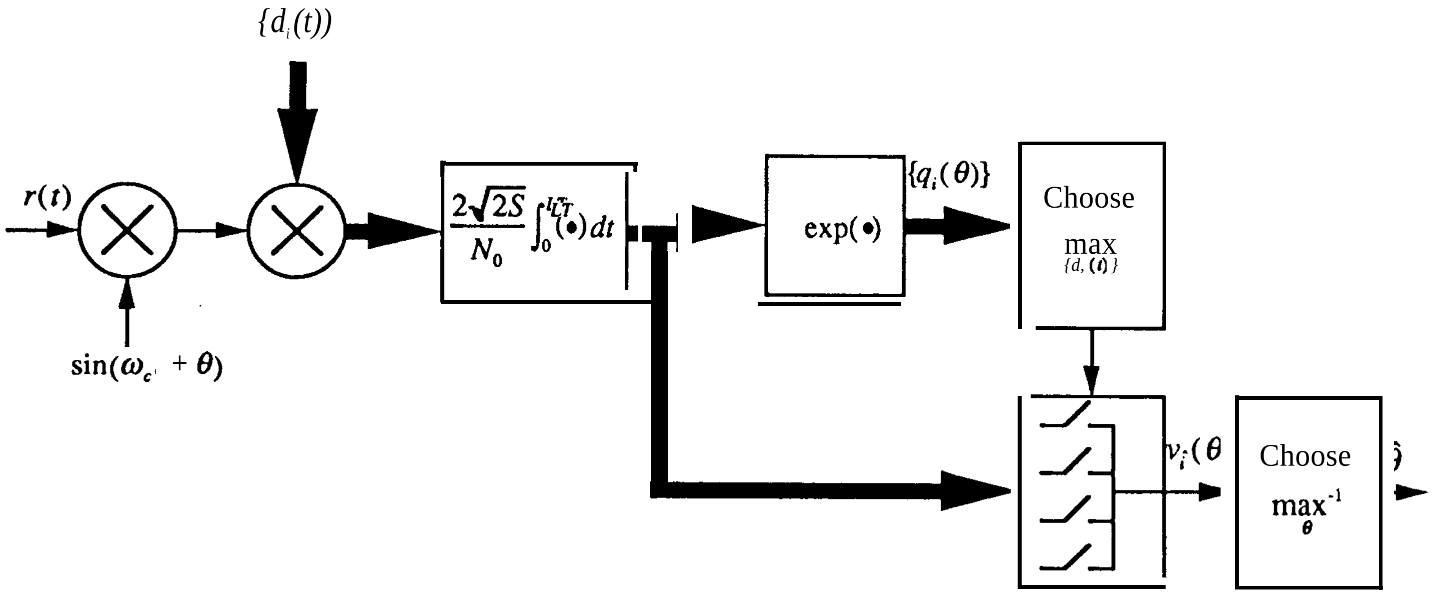

e) ML Open Loop Estimator #4 (Alternate Form)

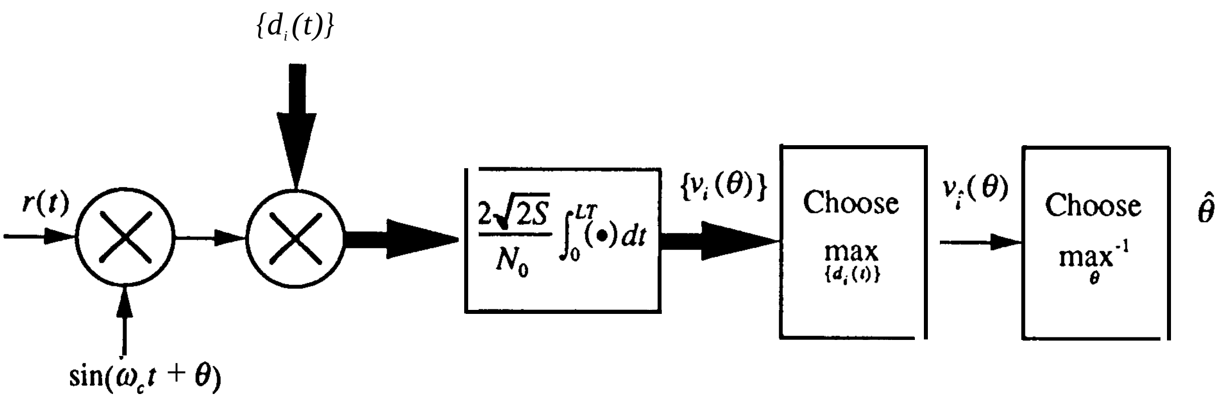

a) ML Closed Loop #1

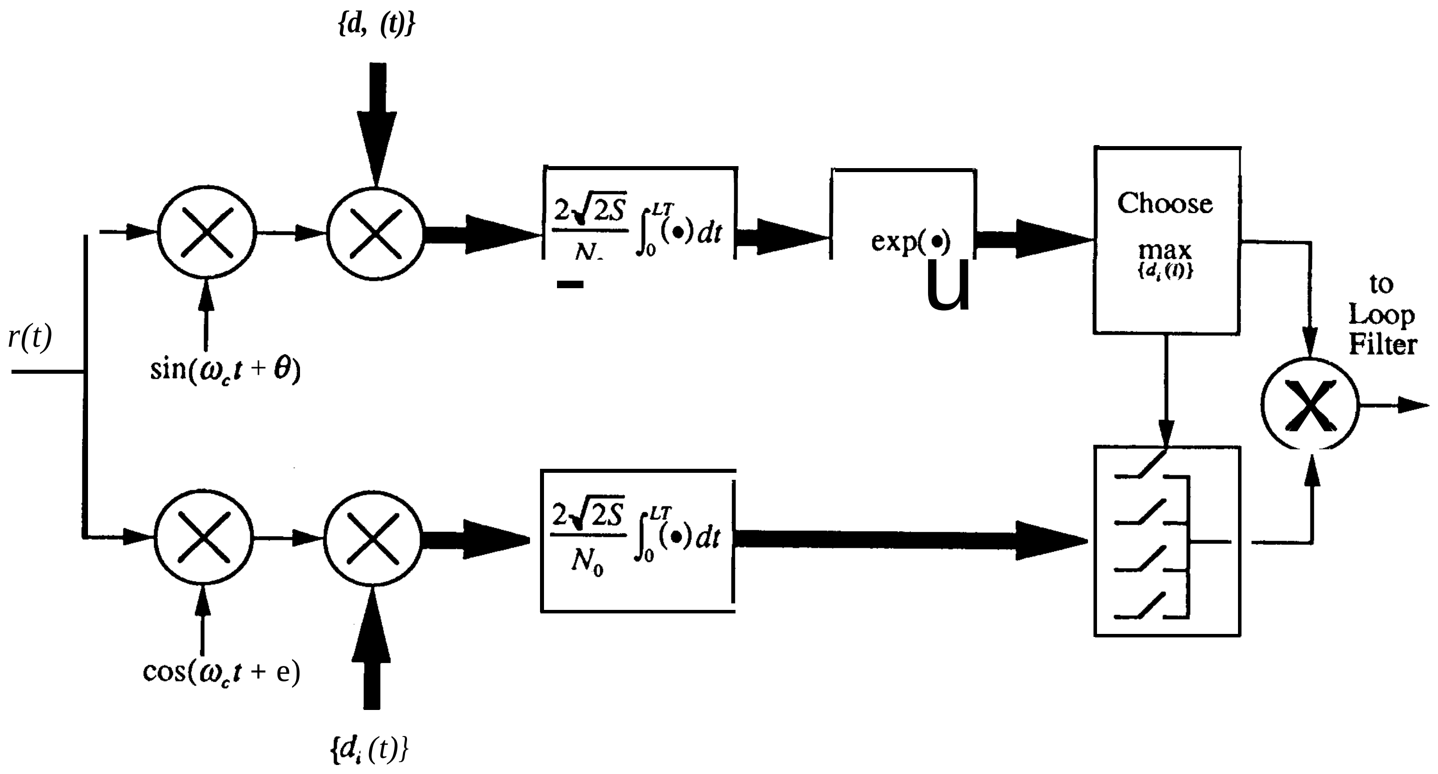

ML Closed Loop #1 (Alternate Form)

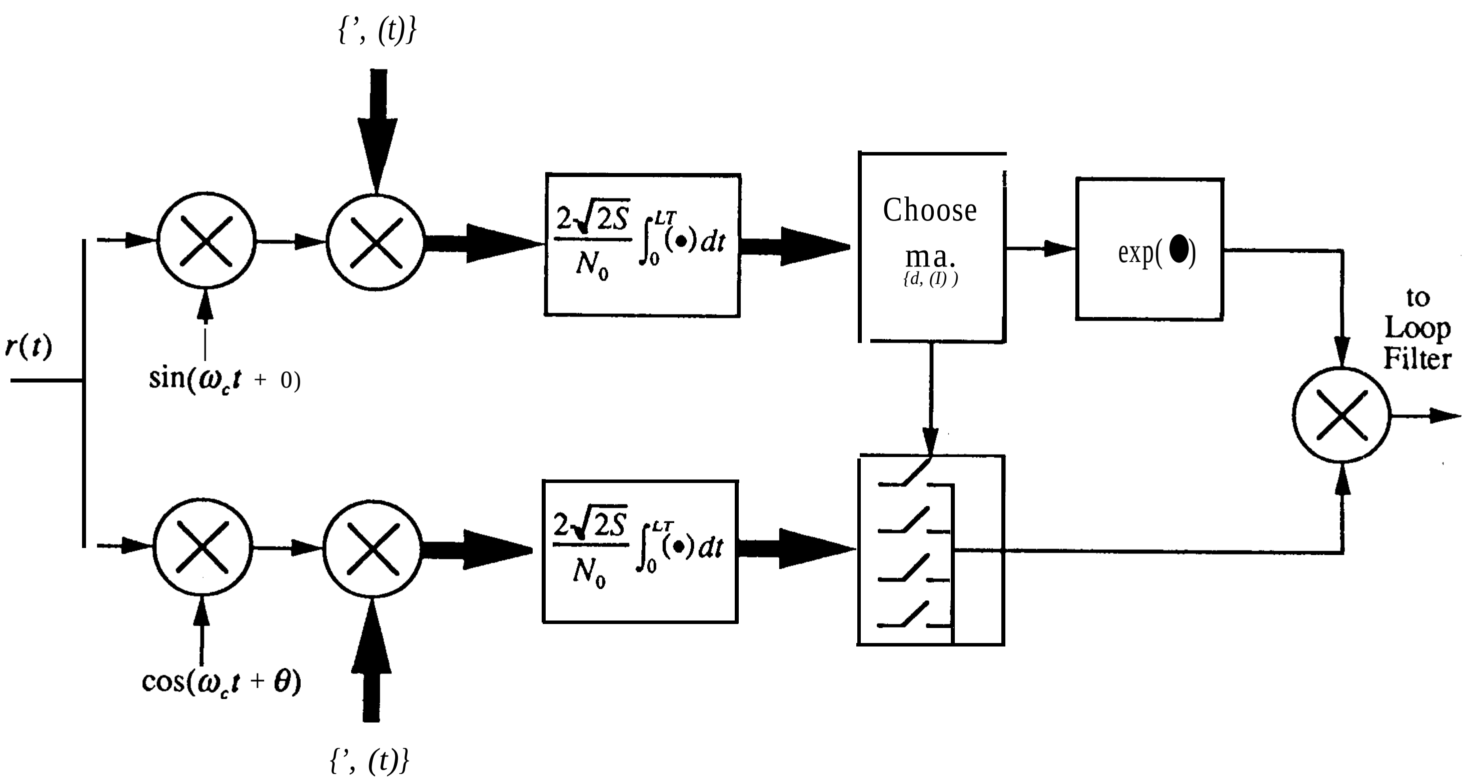

Figure 5. Four ML Closed Loop Carrier Phase Tracking Schemes

b) ML Closed Loop #2

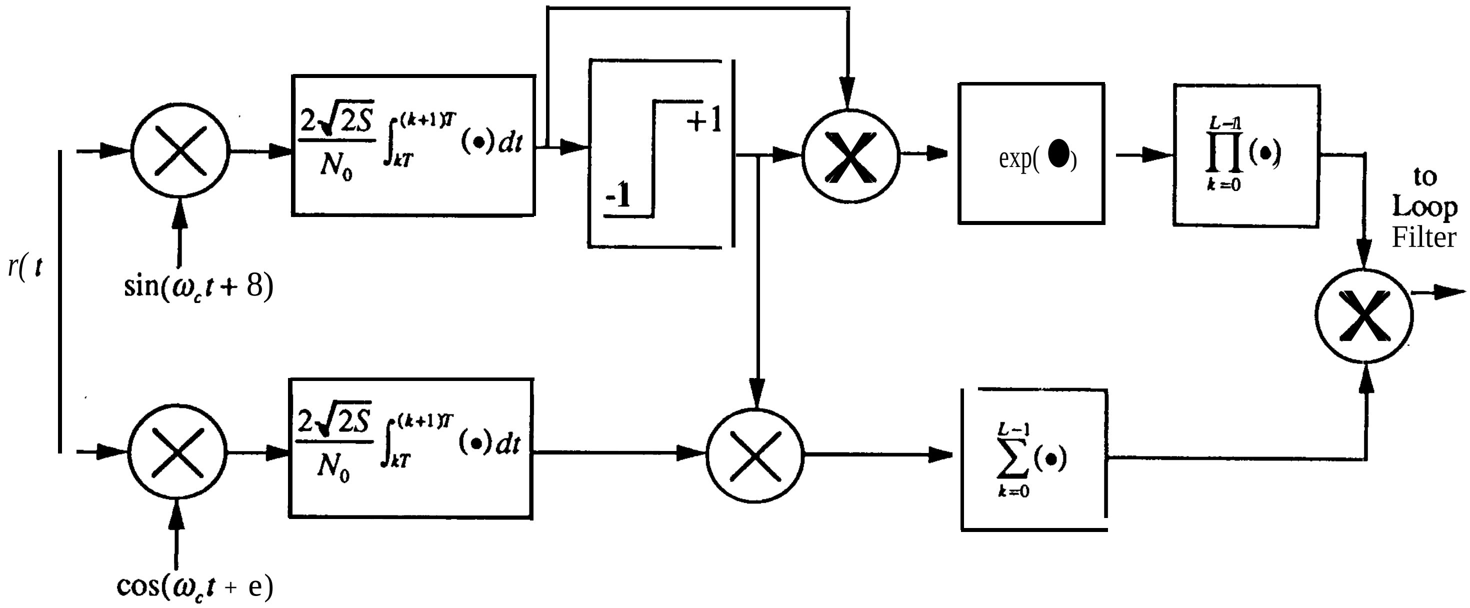

c) ML Closed Loop #3

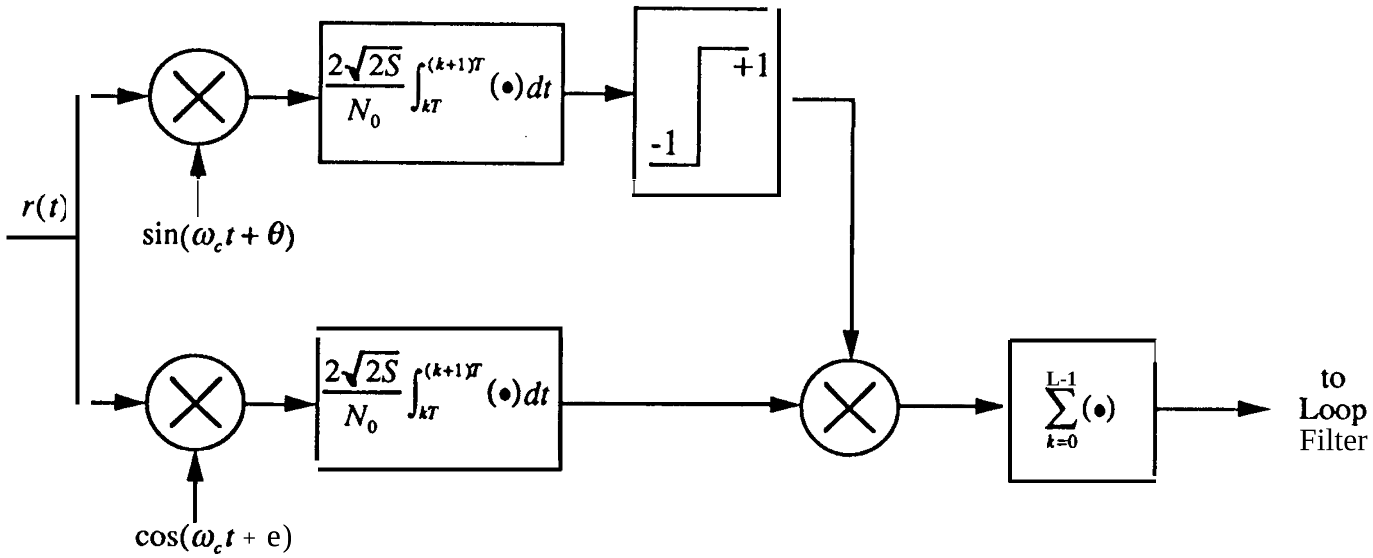

I-Q Polarity-Type Costas Loop

d) ML Closed Loop #4

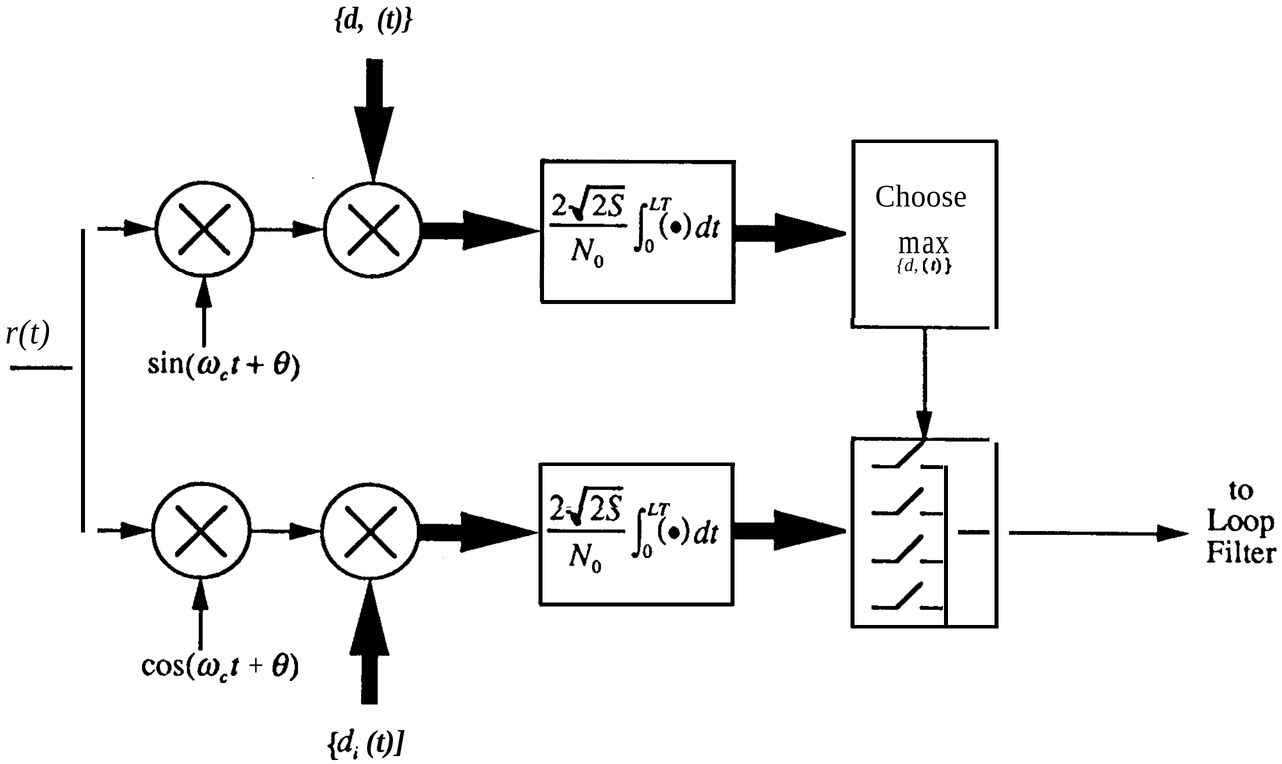

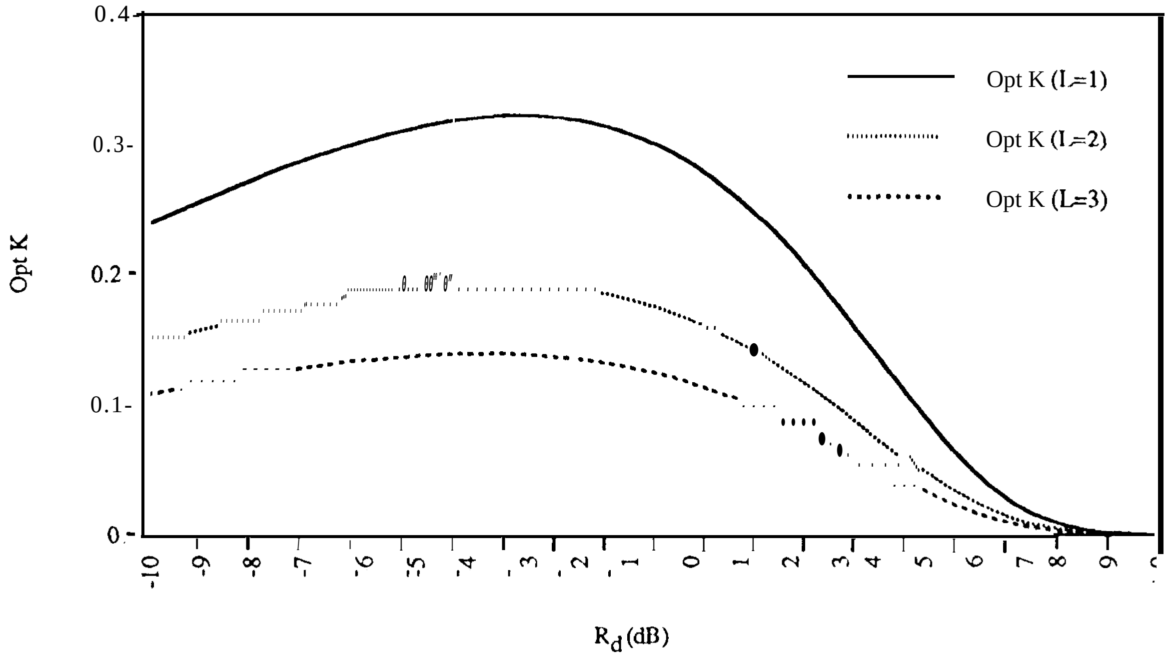

Figure 6. Optimum K versus R_d = ST/N. in dB with Observation Length L as a Parameter for ML Closed Loop #1

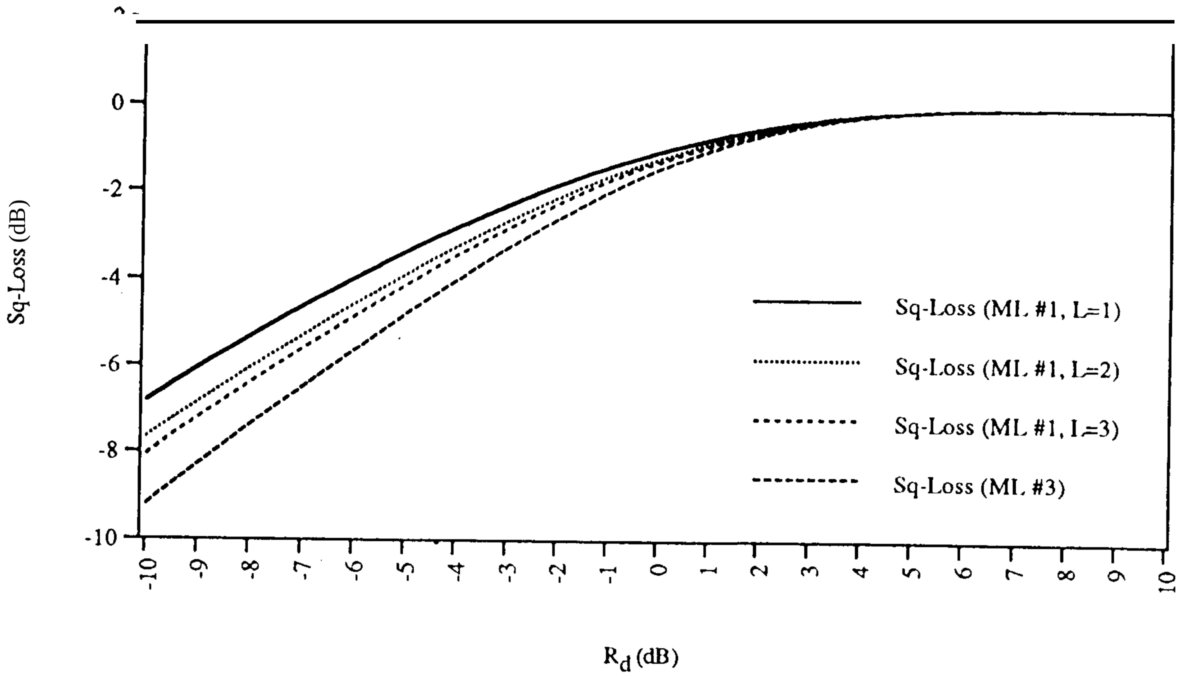

Figure 7. Optimum Squaring Loss versus $R_d = ST/N_o$ in dB with Observation Length L as a Parameter for ML Closed Loop #1

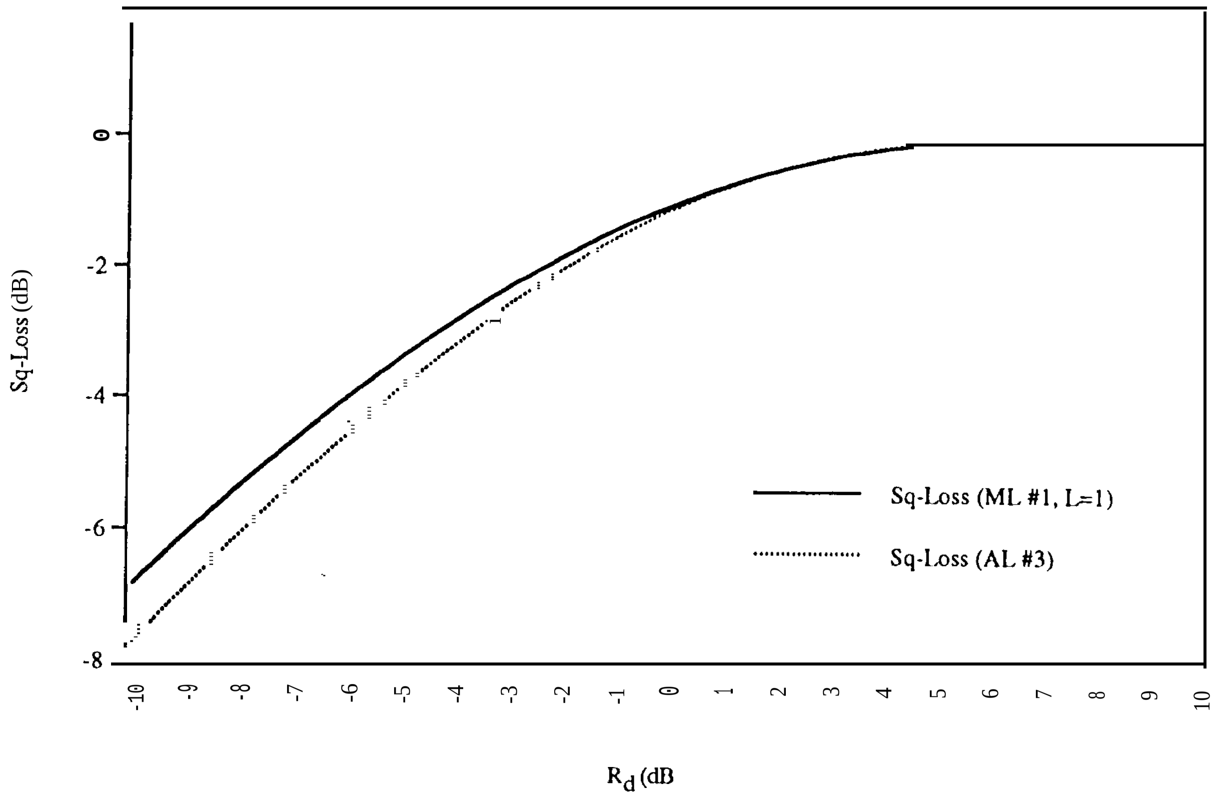

Figure 8. A Comparison of the Squaring Loss Performance of ML Closed Loop #1 and the I-Q MAP Estimation Loop (AL Closed Loop #3)

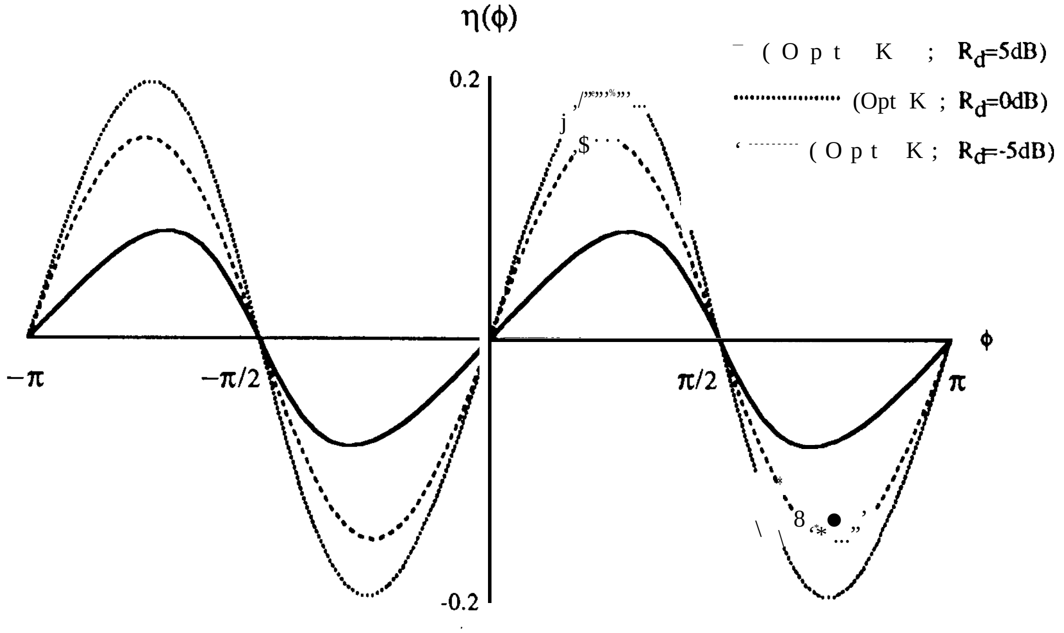

Figure 9. Loop S-Curves for ML Closed Loop #1